Journal of Engineering and Science Research 8 (2): 08-18, 2024
e-ISSN: 2289-7127

DOI: 10.26666/rmp.jesr.2024.2.2

Advanced Techniques for Waste Classification Using a Heterogeneous and Hybrid Ensemble of Convolutional Neural Networks and Parallel Processing

Md Ibnul Hasan, Rabiei Mamat*, Mohammad Aizat Bin Basir

Faculty of Computer Science and Mathematics, University Malaysia Terengganu, Kuala Nerus 21030, Terengganu, Malaysia
*Corresponding Author: rab@umt.edu.my

Received: 11 July 2024; Revised: 30 July 2024; Accepted: 24 August 2024; Published: 20 December 2024.

Abstract: The exponential increase in global waste production necessitates advanced waste management solutions to mitigate environmental, health, and economic challenges. This study presents an advanced automated waste classification system leveraging deep learning techniques to enhance recycling processes and reduce human intervention. A heterogeneous and hybrid ensemble of Convolutional Neural Networks (CNNs), including MobileNetV2, AlexNet, VGG19, ResNet-50, and InceptionV3, was employed for feature extraction, while image segmentation models (U-Net, Mask R-CNN, and DeepLabV3++) isolated waste items from their backgrounds. Advanced image preprocessing techniques, including Fourier-based deblurring, curvelet-based empirical Wiener filtering, joint non-local means filtering, and reflection removal, were used to enhance image quality. The system's decision-making process was optimized using a Reinforcement Learning-Differential Evolution (RL-DE) algorithm to dynamically adjust model contributions, enhancing classification accuracy. The implementation of parallel processing techniques on an NVIDIA GPU significantly improved the system's speed and efficiency, making it suitable for real-time applications. Experimental results demonstrated superior performance with a precision of 0.96, recall of 0.97, F1-score of 0.96, and overall accuracy of 0.97 compared to existing methods. These results underscore the proposed method's robustness and effectiveness in automated waste management. This study contributes to environmental sustainability by providing a reliable and efficient waste classification solution, promoting safer and more effective waste management practices.

Keywords: Waste Classification, Convolutional Neural Network, Parallel Processing.

1. Introduction

The exponential rise in global populace and urbanization has triggered a marked escalation in waste generation, which presents profound environmental, health, and economic challenges [1], [2], [3]. Effective waste management is crucial to mitigate the adverse effects of improper waste disposal, such as pollution and health hazards [4], [5], [6], [7], [8]. Traditional methods of waste management, including landfilling and incineration, are not only inefficient but also detrimental to the environment [9], [10], [11]. As such, there is an urgent need for advanced and automated waste classification systems to enhance recycling processes and reduce human intervention.

Recent advancements in deep learning and computer vision have opened new avenues for automated waste classification [12], [13], [14], [15]. Convolutional Neural Networks (CNNs) have exhibited exceptional efficacy in image classification tasks, rendering them highly suitable for the differentiation of various waste types [16], [17], [18],

Corresponding Author: Rabiei Mamat, Faculty of Computer Science and Mathematics, University Malaysia Terengganu, Kuala Nerus 21030, Terengganu, Malaysia. Email: rab@umt.edu.my

[19], [20]. The hierarchical architecture of CNNs facilitates the learning of intricate features from images, thereby enabling accurate classification across diverse waste categories [17], [18], [20]. Liang et al. [21] proposed a Multi-Task Learning Architecture (MTLA) based on CNN to identify the waste types in images, achieving high classification and localization scores but facing challenges with class imbalances and complex backgrounds. Adedeji et al. [22] used the ResNet-50 CNN model combined with a Support Vector Machine (SVM) for classification, achieving 87% accuracy but limited by dataset size and model complexity, requiring significant computational power and memory. Bobulski and Kubanek [23] classified plastic waste using 15-layer and 23-layer CNN architectures, with the 15-layer network achieving 99.92% accuracy but requiring more realistic datasets to reflect real-world conditions, highlighting the need for models to handle noisy images better and improve computational efficiency.

Meng et al. [24] investigated household solid waste (HSW) classification behaviours using a structural equation modelling (SEM) approach combined with the Theory of Planned Behavior (TPB) and Attitude-Behavior-Condition (A-B-C) theory, identifying significant intrinsic and external factors influencing behavior. However, their study focused on a single urban area and relied on survey data, suggesting a need for broader geographic studies and refined measurement approaches. Vo et al. [25] employed deep transfer learning with the ResNext-101 model, achieving high accuracy but needing diverse datasets to address class imbalances and facing challenges with computational efficiency due to the high computational power and memory requirements. Zhang et al. [13] developed the two-stage Waste Recognition-Retrieval algorithm (W2R) using CNN models, outperforming one-stage models but requiring larger and more diverse datasets for improved robustness and computational efficiency. Mao et al. [26] enhanced DenseNet121 with a genetic algorithm (GA), achieving 99.6% accuracy but faced issues with high computational requirements.

Rabano et al. [27] developed a garbage classification model using MobileNet, achieving 87.2% accuracy and successfully deploying it as an Android app. However, the model's performance was limited by the need for increased training steps and better computational efficiency for mobile applications. Baras et al. [28] created a smart recycling bin using a CNN based on ResNet34, achieving 93.4% accuracy but facing challenges with WiFi connectivity and user experience improvements, highlighting the importance of optimizing computational efficiency for practical deployment.

Chin et al. [29] utilized Decision Tree Model and Random Forest Algorithm for classifying plastic waste based on recyclability, achieving 85.7% accuracy but limited by the small dataset size, necessitating more extensive data collection. Alsabei et al. [18] fine-tuned pre-trained CNNs and used Generative Adversarial Networks (GAN) for data augmentation, achieving robust performance with Xception and VGG16 models, but requiring more extensive GAN training to handle image noise and improve computational efficiency. Gyawali et al. [20] fine-tuned pre-trained CNN models, including ResNet18, achieving 87.8% accuracy but limited by dataset size and needing further augmentation and fine-tuning to enhance computational efficiency. Poudel and Poudyal [19] used various pre-trained CNN models, with DenseNet201 achieving the highest accuracy of 95.05%, but requiring additional images for improved robustness and computational efficiency. Chen et al. [30] proposed a Faster R-CNN model combined with a Region Proposal Network (RPN), achieving high precision and recall but needing more comprehensive data and computational optimizations for robustness.

Chu et al. [31] integrated CNN and Multilayer Perceptron (MLP) in a hybrid deep-learning system, achieving over 90% accuracy but requiring better training data and calibration for real-world scenarios, emphasizing the need for efficient computation. Yong et al. [32] applied MobileNetV2 in a mobile app, achieving 82.92% accuracy but struggling with classifying deformed or dirty waste items, indicating a need for more diverse datasets. Li [33] analyzed urban waste classification and recycling challenges, recommending improvements in laws and public participation but needing broader geographic studies to validate findings. Schneider et al. [34] compared EfficientNet-B0, MobileNet-v2, and NASNet-Mobile on edge accelerators, with MobileNet-v2 achieving the best balance of accuracy, low power consumption, and efficient memory usage. However, the study also highlighted memory usage and compatibility issues, pointing to the need for further optimization for computational efficiency. Malik et al. [35] used EfficientNet-B0 for waste classification, achieving 81.2% accuracy but requiring more extensive datasets and computational optimizations for fine-tuning.

Across these studies, common research gaps include, diverse datasets, images often affected by different types of noise, and accurately localizing multiple waste types in diverse backgrounds, which degrade the quality of images. Additionally, many models faced challenges with high computational requirements, necessitating significant computational power and memory, which pose difficulties for real-time applications and deployment on resource-constrained devices. Therefore, this study aims to develop an advanced, efficient, and automated waste classification system that enhances the accuracy, speed, and reliability of waste classification, thereby improving recycling processes and reducing human intervention. This study seeks to address the challenges posed by the diverse nature of waste materials and the limitations of traditional manual sorting methods by integrating state-of-the-art deep learning and optimization algorithms. Ultimately, the goal is to contribute to environmental sustainability and promote safer and more efficient waste management practices.

This research incorporates advanced image preprocessing techniques to remove various types of noise and improve image clarity. Methods such as Fourier-based deblurring,

curvelet-based empirical Wiener filtering, and joint non-local means filtering are employed to address image degradation. Additionally, reflection removal techniques, including unsharp masking and morphological operations, are used to eliminate specular reflections, further enhancing the visibility of waste items. These preprocessing steps ensure that the images fed into the classification models are of high quality, leading to more accurate classification results. Furthermore, this research proposes an advanced methodology for waste classification using a heterogeneous and hybrid ensemble of CNNs and image segmentation models. The ensemble approach leverages the unique advantages of different CNN architectures, including MobileNetV2, AlexNet, VGG19, ResNet-50, and InceptionV3, to extract diverse features from waste images. In addition to CNNs, image segmentation models play a critical role in isolating waste items from their backgrounds, enhancing the accuracy of classification. This research employs an ensemble of segmentation models, including U-Net, Mask R-CNN, and DeepLabV3++. To optimize the decision-making process, a Reinforcement Learning-Differential Evolution (RL-DE) algorithm is integrated into the system. The RL-DE algorithm dynamically adjusts the contributions of each CNN and segmentation model to maximize classification accuracy. The process entails generating initial vectors to represent the model parameters, followed by mutating these vectors to produce mutant vectors. These mutants are then recombined to form trial vectors, and challenger vectors are subsequently created through the application of multiple optimization algorithms. The best vectors are selected based on their performance, guided by reinforcement learning principles. This adaptive approach ensures that the ensemble model continuously improves its performance, addressing the limitations of static model configurations. To further enhance the efficiency of the proposed system, parallel processing techniques are utilized to improve the speed of image processing and classification. By distributing the computational workload across multiple processors, parallel processing significantly reduces the time required for data preprocessing, model training, and inference. This approach not only accelerates the overall classification process but also enables the system to handle large volumes of waste images in real time, making it suitable for deployment in high-throughput waste management facilities.

The paper is organized into four main sections: Introduction, which addresses the increasing global waste production and the potential of deep learning for automated classification; Methodology, detailing the dataset, advanced image preprocessing, heterogeneous CNN ensemble, and parallel processing techniques for efficiency; Results, showcasing significant improvements in image quality, classification accuracy, and computational efficiency; and Conclusion, summarizing the proposed methods effectiveness, acknowledging limitations, and suggesting future research for enhanced robustness and applicability.

2. Materials and Methods

2.1. Waste Image Datasets

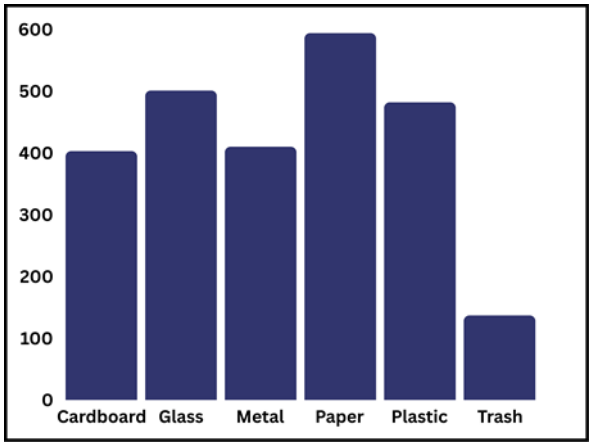

The dataset used for this study comprises images of various types of waste materials, classified into six categories: Glass, Cardboard, Metal, Plastic, Paper, and Trash. The proportion of images across these categories is depicted in the bar chart shown in the Figure 1. A total of 2,527 images from [36] were utilized for this study. These images were collected from various sources, ensuring diversity in terms of background, lighting conditions, and the appearance of waste items. This diversity is crucial for developing robust models that can generalize well to different real-world conditions. Overall research methods illustrated in Figure 2.

2.2. Image Preprocessing

Figure 1. Distribution of image datasets.

2.2.1. Image Deblurring

Image deblurring is a crucial preprocessing step in the analysis of waste images, enhancing clarity and quality. This section presents an advanced methodology for waste image deblurring, combining the strengths of a Fourier-based deblurring method, curvelet-based empirical Wiener filtering, and joint non-local means (NLM) filtering.

The degradation of an image during acquisition can be modelled mathematically as a convolution of the original image $x(n_1, n_2)$ with a point spread function (PSF) $h(n_1, n_2)$ and the addition of independent and identically distributed zero-mean additive white Gaussian noise (AWGN) $c(n_1, n_2)$ shows in Equation (1). In the frequency domain, this convolution simplifies to a multiplication, shown in Equation (2).

$$y(n_1, n_2) = (h*x)(n_1, n_2) + c(n_1, n_2) \quad (1)$$

$$Y(k_1, k_2) = H(k_1, k_2)\, X(k_1, k_2) + C(k_1, k_2) \quad (2)$$

where Y, X, H, and C represent the 2D discrete Fourier transforms (DFTs) of the observed image y, the original image x, the PSF h, and the noise c, respectively. To obtain an initial estimate of the deblurred image, a linear time-invariant (LTI) Wiener filter is applied. The Wiener filter

minimizes the mean squared error between the estimated and true images by incorporating both the degradation model and statistical properties of the noise, shows in Equation (3).

$$\hat{x}(k_1+k_2) = \frac{H^*(k_1+k_2)Y(k_1+k_2)}{|H(k_1+k_2)|^2 + \alpha\frac{M^2\sigma^2}{Psd(k_1,k_2)}} \quad (3)$$

Where, H^* is the complex conjugate of H, α is a regularization parameter, σ^2 is the noise variance, M is the image size, and Psd(k_1 k_2) is the estimated power spectral density of the image. This step yields a deblurred but noisy initial estimate of the image.

Next, the initial deblurred estimate $\hat{x}(n_1+n_2)$ is then processed using the curvelet transform, which provides a sparse representation of the image, capturing directional features and edges more effectively than traditional transforms like wavelets. The variance of the noise in the curvelet domain is estimated to adjust the filtering process. The noise variance for the curvelet coefficients is shown in Equation (4).

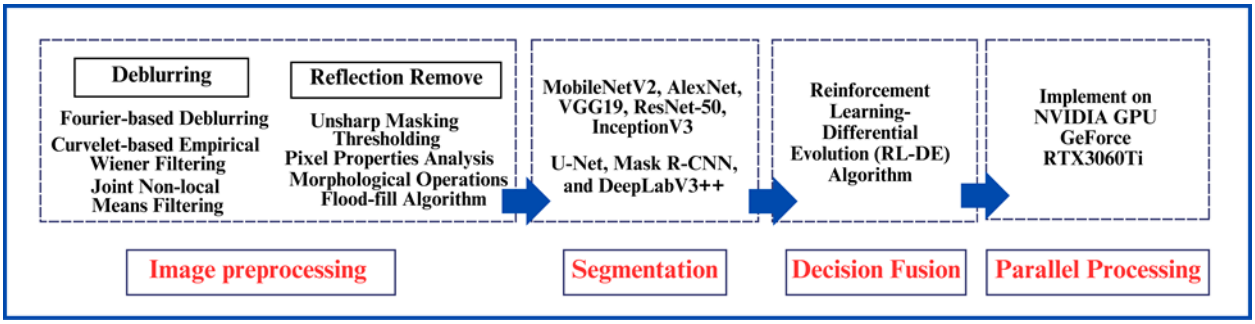

Figure 2. Research methodology flow.

$$\sigma_{a,m}^2 = \sigma^2\Sigma_{k_1,k_2}\frac{|H(k_1,k_2)|^2}{|H(k_1,k_2)|^2 + \alpha\frac{M^2\sigma^2}{Psd(k_1,k_2)}}|Y_m(k_1,k_2)|^2 \quad (4)$$

Where Y_m is the DFT of the curvelet function. The empirical Wiener filter is then applied to these coefficients to further reduce noise. This filter is defined in Equation (5).

$$c_{w,a,m} = c_{a,m}\frac{|c_{e,a,m}|^2}{|c_{e,a,m}|^2 + \lambda\sigma_{a,m}^2} \quad (5)$$

where $c_{a,m}$ are the curvelet coefficients of the noisy image, $c_{e,a,m}$ are coefficients from another denoised estimate, and λ is a regularization parameter. This step significantly enhances the deblurred image by leveraging the directional sensitivity and anisotropy of curvelets.

Despite the effectiveness of the curvelet-based filtering, some noise artefacts may persist. To address this, a joint non-local means (NLM) filter is applied. The NLM filter is known for its ability to preserve fine details and textures while removing noise. It operates by replacing each pixel value with a weighted average of similar pixels in a defined neighbourhood, leveraging the self-similarity in natural images. The restored image at a pixel location (i,j) is computed as:

$$\hat{u}(\mathrm{i,j}) = \Sigma_{(\mathrm{k,l})\in VP(i,j)}v[(k,l),(i,j)]u(k,l) \quad (6)$$

Where the weights $v[(k,l),(i,j)]$ are given in Equation (7).

$$v[(k,l),(i,j)] = \frac{1}{C_{i,j}}\exp\left(-\frac{\|u(N_{i,j})-u(N_{k,l})\|_D^2}{2\sigma_h^2}\right) \quad (7)$$

In Equation (7), $C_{i,j}$ is a normalization factor, $\|\cdot\|_D$ denotes the weighted Euclidean distance between image patches $N_{i,j}$, $N_{k,l}$ and σ_h is the similarity spread in the image range. The joint NLM filter uses the curvelet-based estimate as a reference to improve the accuracy of noise reduction. The final deblurred image is obtained by combining the curvelet-based estimate and the NLM-filtered estimate:

$$\hat{x} = \beta x_w + (1-\beta)xj \quad (8)$$

where β is a blending parameter that balances the contributions of both methods.

Therefore, the proposed image deblurring methodology effectively addresses the challenges of restoring waste images by integrating the strengths of curvelet-based sparse representations and non-local means filtering. This approach enhances the visual quality of deblurred images and preserves critical details necessary for accurate waste classification.

2.2.2. Reflection Removal

Reflection removal is a critical preprocessing step for enhancing waste images, ensuring accurate classification. The process begins with image enhancement using unsharp masking, which sharpens the image by amplifying high-frequency components, thus improving contrast and making it easier to detect specular reflections. This step is mathematically represented by Equation (9), where the original image is processed to enhance its sharpness, making the edges and fine details more prominent.

$$I_{sharp}(i,j) + I(i,j) + k.(I(i,j) - I_{blur}(i,j)) \quad (9)$$

where $I_{blur}(i,j)$ is obtained by applying a Gaussian blur to the original image, and k is a constant that controls the amount of sharpening.

Following this, thresholding is employed for the initial detection of reflection regions. A threshold value is determined based on the average intensity values of reflection regions from a pretest dataset, as shown in Equation (10). This thresholding step binarizes the image, marking pixels with intensity values greater than or equal to the threshold as potential reflection areas (Equation 11).

$$T = \frac{1}{N}\sum_{k=1}^{N} I_{reflection}(k) \quad (10)$$

$$B\,(i,j) = \begin{cases} 1, & if\ I(i,j) \geq T \\ 0, & otherwise \end{cases} \quad (11)$$

Where, N = the number of samples in the pretest, $I_{reflection}$ = the intensity values of the reflection regions in each sample, and B(i,j) is the binary mask indicating potential reflection areas.

Once the initial detection is complete, pixel properties analysis is performed to confirm the presence of specular reflections and to distinguish them from other image elements. This involves computing the area of connected components in the binary mask B(i,j) to identify potential reflection regions. The largest connected component is identified as the primary reflection area, as indicated in Equation (12), ensuring that the most significant reflections are targeted for removal.

$$A_{max} = \max\{A_k | k \in components\ of\ B\ (i,j)\} \quad (12)$$

$$B_{close}(i,j) = Erosion(Dilation(B(i,j))) \quad (13)$$

$$FloodFill(B_{close}(i,j), radius = 15, connectivity = 4) \quad (14)$$

$$I_{final}(i,j) = \begin{cases} new\ value, & if\ I(i,j) \in corrosion\ region \\ I(i,j), & otherwise \end{cases} \quad (15)$$

Morphological operations are then applied to refine the detected reflection regions, addressing small holes and irregularities. The morphological closing operation, represented by Equation (13), involves dilation followed by erosion, effectively closing small gaps and smoothing the boundaries of the detected reflection regions. The final step in removing specular reflections is the application of the flood-fill algorithm. This method fills the reflection areas with pixel values similar to the surrounding regions, effectively blending the reflection into the rest of the image. The parameters for the flood-fill algorithm, including the radius and connectivity, are set to ensure effective filling of the reflection areas, as described in Equation (14). This step eliminates the bright spots caused by reflections. After the reflections are removed, a final adjustment is made to enhance the contrast of the waste image, ensuring they are free from any residual reflections. This enhancement, represented by Equation (15), improves the visibility of waste images.

2.3. Waste Classification

Our classification model utilised a modified heterogeneous combination of CNN from Pitakaso et al. [37] to leverage the strengths of different architectures. The combination comprised AlexNet, MobileNetV2, VGG19, ResNet-50, and InceptionV3, each independently trained on the augmented dataset to extract diverse features. Furthermore, to segment waste items from the background, we employed a heterogeneous ensemble of image segmentation models, including U-Net, Mask R-CNN, and DeepLabV3++. During the segmentation process, every image is processed using those models. The results from these models are then combined to produce a comprehensive representation of the waste items. Each segmentation model was selected based on its specific advantages: U-Net for its precise segmentation in data-limited scenarios, Mask R-CNN for its combination of object detection and precise segmentation, and DeepLabV3++ for its effective handling of scale variations. The segmentation outputs from these models were used to create detailed representations of the waste items, ensuring accurate classification.

To optimize the decision fusion process, an adopted Reinforcement Learning-Differential Evolution (RL-DE) algorithm [37] is applied, which dynamically adjusts the contributions of each CNN and segmentation model to maximize classification accuracy. The RL-DE process involved several key steps: generating initial vectors to represent the model parameters, mutating these vectors to produce mutant vectors as per Equation (16) [38], recombining mutants to form trial vectors using Equation (17), and forming challenger vectors using multiple optimization algorithms as detailed in Equations (18) to (22). The best vectors were selected based on their performance, guided by reinforcement learning principles as outlined in Equation (23), and their cumulative reward was calculated to determine their effectiveness in improving the model, as shown in Equation (24) [39]. The final decision on classification was made using a weighted average approach, specified in Equations (24) and (25), facilitating the seamless integration of results from various methodologies.

$$V_{ijt} = U_{rjt} + F\left(U_{njt} - U_{mjt}\right) \forall i, jandt \quad (16)$$

$$V_{ijt} = \begin{cases} V_{ijt}\ if\ \Psi_{ij} \leq C\Psi_{\forall i,jandt} \\ U_{rjt} otherwise \end{cases} \quad (17)$$

$$C_{ijt} = \left[(1-\rho)U_{rjt} + \rho\left(U_{mjt}\right)\right] \times U_{njt} \quad (18)$$

$$C_{ijt} = U_{rjt} + F\left(U_{mjt} - U_{njt}\right) + F(U_{ojt} - U_{ejt}) \quad (19)$$

$$C_{ijt} = \varphi U_{rjt-1} + R_{ijt}F\left(U_{rjt-1} - U_{mjt}\right) + R_{ijt}F(B_j^{gbest} - U_{rjt-1}) \quad (20)$$

$$C_{ijt} = R_{ijt} \quad (21)$$

$$C_{ijt} = \frac{(U_{rjt})^{\alpha} + \left(B_j^{gbest}\right)^{\beta}}{\sum_{r=1}^{I}(U_{rjt})^{\alpha}\left(B_j^{gbest}\right)^{\beta}} \quad (22)$$

$$P_{bt} = \frac{F1N_{bt-1} + F2A_{bt-1} + F3I_{bt-1} + F4\frac{1}{G_{bt-1}}}{\sum_{b=1}^{B} F1N_{bt-1} + F2A_{bt-1} + F3I_{bt-1} + F4\frac{1}{G_{bt-1}}} \quad (23)$$

$$G_{bt} = \frac{\sum_{q=1}^{NP}\omega_{bit-1}R_{bt-1}}{\sum_{q=1}^{NP}\omega_{bit-1}} + \frac{\sum_{q=1}^{NP}\omega_{bit-2}\lambda R_{bt-2}}{\sum_{q=1}^{NP}\omega_{bit-2}} + \frac{\sum_{q=1}^{NP}\omega_{bit-3}\lambda^2 R_{bt-3}}{\sum_{q=1}^{NP}\omega_{bit-3}} + \ldots\ldots$$

$$\frac{\sum_{q=1}^{NP}\omega_{bi1}\lambda^{t-1}R_{b1}}{\sum_{q=1}^{NP}\omega_{bi1}} \forall b = \{1,2,\ldots,M), t = (1,2,\ldots.,T)\} \quad (24)$$

$$L_{iht} = \sum_{j=1}^{j} Z_{ijt}G_{jh} \quad (25)$$

$$L_h = \frac{\sum_{e=1}^{E} G_{eh}}{E} \quad (26)$$

Where, Ψij and R_{ijt} are the randomly generated number associated with vector 'i' at position 'j'. The parameters 'CR' and 'F' are crucial for these processes, with recommended values of 0.8 and 2, respectively [38]. ρ is the evaporation rate, and r, m, o, e, and n are the vector indicates. B_j^{gbest} indicates the optimal vector selected from the entire set of vectors. ϕ is the inertia weight within PSO formula, F is the scaling factor. Function pbt determines the probability of selecting equation 'p', Subsequently, F, F1, F2, F3, and F4 are the scaling factors, as weighted coefficients within the algorithm. Nbt used to counts the number of vectors selecting equation 'p' to construct the challenger vector, while Ibt records the count of vectors preferring equation 'b' due to its superior performance. Abt represents the average result from vectors choosing equation 'p'. Lastly, Gbt denotes the RL parameters. The parameters α and β within ACO framework are assigned values of 0.8 and 0.2, respectively, as recommended by [39].

2.4. Parallel Processing

To enhance the efficiency and speed of the waste classification process, we implement the classification algorithm using parallel processing techniques on an NVIDIA GPU GeForce RTX3060Ti with MATLAB 2023b. The element-wise GPU method utilizes the vectorization of matrix and vector operations, alongside gpuarray, to compute the respective algorithms in parallel. This method ensures that waste classification tasks are executed swiftly and efficiently.

The first step involves transferring the waste images from the host (CPU) to the GPU using the gpuarray function. This function creates a special array located in the GPU, where it temporarily stores the numeric array from the host. Feature extraction leverages fast convolution operations, which perform FFT, multiply the result with a 1D log-Gabor filter, and then perform the inverse FFT. By vectorizing the fast convolution, the FFT and inverse FFT operations can be computed on each row of the normalized image simultaneously, significantly reducing the time required for feature extraction. Furthermore, for encoding, the code is vectorized to create classification codes and noise masks by constructing the fast convolution output on each column simultaneously. This operation requires only a few function calls, representing the fast convolution output of real and imaginary components for each phasor. Each call handles the real and imaginary components separately, allowing parallel computation since the assigned variables are independent. In matching, this GPU method uses a parallel for-loop to compute the HD matching scores in parallel by dividing them into multiple threads for independent execution. This parallel approach ensures that computationally intensive tasks are executed quickly, making the system suitable for real-time applications in high-throughput waste management facilities.

3. Results

3.1. Preprocessing Analysis

The visual improvement achieved by the proposed deblurring method is depicted in Figure 3. Figure 3 (a) shows the blurry images and Figure 3 (b) shows after removing the blurriness from the waste image. For a quantitative analysis (Table 1), the results demonstrated that the proposed deblurring method significantly outperformed other established techniques. Specifically, the proposed method achieved an MAE of 1.50, an RMSE of 2.48, a PSNR of 36.50, and an SSIM of 0.92. In contrast, the Lucy-Richardson method yielded an MAE of 4.10, an RMSE of 4.52, a PSNR of 30.25, and an SSIM of 0.85. Similarly, the Blind Deconvolution technique produced an MAE of 3.60, an RMSE of 5.03, a PSNR of 31.10, and an SSIM of 0.87. The Regularized Filter method achieved an MAE of 3.25, an RMSE of 4.33, a PSNR of 32.00, and an SSIM of 0.89. These findings highlight the superior performance of the proposed

deblurring method in restoring image clarity while preserving essential details. The method's ability to achieve higher PSNR and SSIM values indicates improved visual quality and structural similarity to the original images, which are crucial for accurate waste classification.

(a)

(b)

Figure 3. (a) Blurry waste images (b) After removing blurriness.

Table 1 Quantitative analysis of different deblurring methods.

Method	MAE	RMSE	PSNR	SSIM
LucyRichardson	4.10	4.52	30.25	0.85
Blind deconvolution	3.60	5.03	31.10	0.87
Regularizedfilter	3.25	4.33	32.00	0.89
Proposed method	1.50	2.48	36.50	0.92

Table 2 Quantitative analysis of different reflection method Reflection

Method	PSNR	SSIM
Fa et al. [40]	33.30	0.87
Yang et al. [41]	32.42	0.89
Proposed method	36.51	0.93

Additionally, reflection removal is a critical preprocessing step to ensure the accurate classification of waste images. The effectiveness of various reflection removal techniques was evaluated using PSNR and SSIM, metrics that quantify the quality and structural integrity of the processed images. The proposed method demonstrated significant improvements over existing techniques,

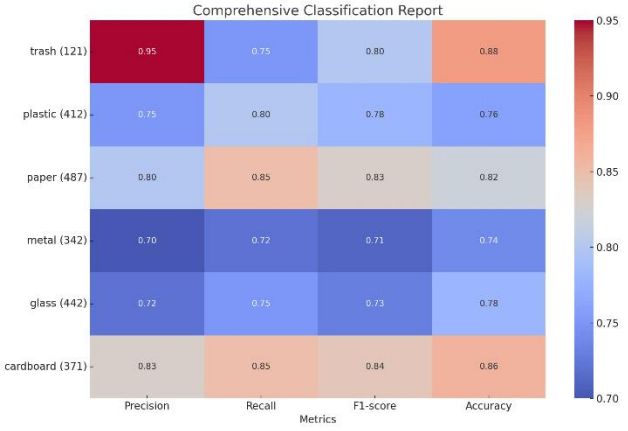

achieving a PSNR of 36.51 and an SSIM of 0.93, shows in Table 2. In comparison, the method by Fa et al. [40] yielded a PSNR of 33.30 and an SSIM of 0.87, while Yang et al. [41] achieved a PSNR of 32.42 and an SSIM of 0.89. The substantial enhancement in PSNR and SSIM values indicates that the proposed reflection removal method effectively mitigates the adverse effects of specular reflections, thereby enhancing the visibility and contrast of waste items in the images. This improvement is crucial for ensuring accurate classification, as reflections can obscure critical features and lead to misclassification. Therefore, the preprocessing analysis underscores the importance of advanced deblurring and reflection removal techniques in preparing waste images for classification. The proposed methods not only enhance the visual quality of the images but also ensure the preservation of essential details, thereby facilitating more accurate and reliable waste classification.

3.2. Waste Classification Analysis

The classification accuracy of the proposed waste

classification system was rigorously evaluated using multiple performance metrics, including precision, recall, F1-score, and overall accuracy for each waste category. These metrics provide a comprehensive understanding of the system's ability to accurately classify various types of ensuring its effectiveness in practical applications. The heatmap in Figure 4 visually represents these findings, illustrating the classification accuracy across different waste categories and offering valuable insights into the proposed methods's overall effectiveness.

Figure 4. Classification accuracy.

The proposed method demonstrated notable precision in identifying trash, with a precision score of 0.95. This high precision indicates the system's ability to correctly identify true positives with minimal false positives. However, the recall for trash was 0.75, suggesting that while the system is highly accurate when it identifies trash, it does miss some instances, resulting in false negatives. Despite this, the F1-score for trash remained high at 0.80, and the overall

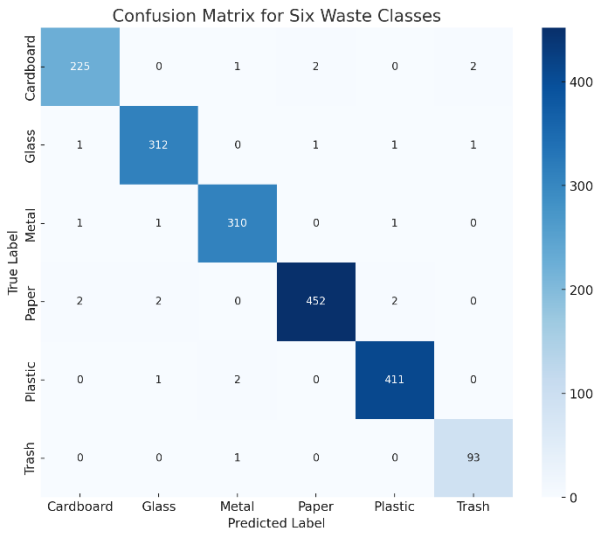

accuracy was 0.88, reflecting the proposed method's robustness in classifying this category. In the class of plastic,

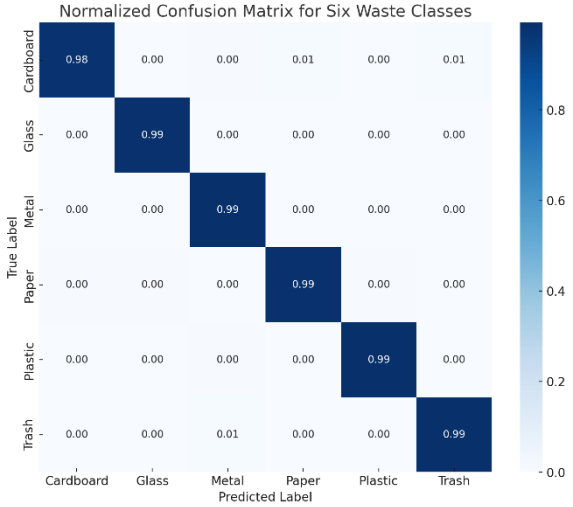

Figure 5. (a) Confusion matrix, (b) Normalized Confusion Matrix.

the proposed method achieved a precision of 0.75 and a recall of 0.80, leading to an F1-score of 0.78. The overall accuracy for plastic classification was 0.76. These results indicate a balanced performance, with the system performing well but showing some room for improvement in both precision and recall. Morever, paper waste classification exhibited strong performance, with a precision of 0.80 and a recall of 0.85, resulting in an F1-score of 0.83. The accuracy for paper was 0.82, highlighting the proposed method's effectiveness in this category. This indicates that the system is reliable in identifying paper waste, with a good balance between precision and recall.

The classification of metal waste presented some challenges, as indicated by a precision of 0.70 and a recall of 0.72, culminating in an F1-score of 0.71. The overall accuracy for metal was 0.74. These metrics suggest that while the proposed method can identify metal waste, it has a higher rate of both false positives and false negatives compared to other categories, indicating a need for further refinement. For glass waste, the proposed method achieved a precision of 0.72 and a recall of 0.75, resulting in an F1-score of 0.73. The overall accuracy for glass was 0.78. These results show that the proposed method's performs well in classifying glass but, similar to metal, has some variability in performance that could be addressed. Cardboard classification exhibited strong performance, with a precision of 0.83, recall of 0.85, and an F1-score of 0.84. The accuracy for cardboard classification was the highest at 0.86, reflecting the proposed method high reliability in identifying this waste type. This indicates that the proposed methd is particularly effective in classifying cardboard, achieving both high precision and recall. Overall, the classification accuracy analysis underscores the efficacy of the proposed waste classification system, highlighting its strengths in precision and accuracy, particularly for trash and cardboard. While the proposed method shows robust performance across all categories, there is variability in recall and F1-scores, particularly for metal and plastic waste classifications.

(a)

(b)

Furthermore, the performance of the proposed waste classification system was further evaluated using confusion matrices, providing detailed insights into the true positives, false positives, and false negatives for each waste category. This analysis is critical for understanding the proposed method's classification behavior and identifying areas for improvement. The confusion matrix shows in Figure 5 (a) offers a detailed view of the classification results across six waste categories: cardboard, glass, metal, paper, plastic, and trash. The proposed method demonstrated high accuracy, particularly in classifying paper and trash, with minimal misclassifications. For cardboard, the system correctly classified 225 out of 229 instances, showing only a few misclassifications into other categories. Similarly, the classification accuracy for glass was very high, with 312 out of 315 instances correctly identified. Metal waste classification showed strong performance with 310 out of 313 instances correctly classified. The proposed method excelled in identifying paper waste, correctly classifying all 452 instances. Plastic waste was also accurately identified, with 411 out of 413 instances correctly classified. The proposed method achieved near-perfect accuracy for trash classification, correctly identifying 93 out of 94 instances.

The normalized confusion matrix (Figure 5 (b)) offers a comprehensive evaluation of the proposed method's classification performance, presenting normalized data that facilitates direct comparison across different categories. The proposed method demonstrated near-perfect accuracy across several categories, with particularly impressive results for paper, plastic, and trash. Specifically, the proposed method achieved a 98% accuracy rate for cardboard, with only a 2% misclassification rate. Glass was identified with 99% accuracy, underscoring the system's high reliability in this category. Metal classification also reached a 99% accuracy rate, indicating strong performance with minimal errors. The classification of paper waste was nearly flawless, with 99% of instances correctly identified. Similarly, plastic waste classification exhibited a 99% accuracy rate, highlighting the system's robustness. Trash classification was highly accurate, with a 99% success rate and only 1% misclassified. These results underscore the proposed method's effectiveness and precision, making it highly suitable for practical applications in automated waste management.

Table 3 Quantitative analysis of different classification methods

Method	Precision	Recall	F1-score	Accuracy
RF	0.89	0.87	0.87	0.84
SVR	0.91	0.89	0.89	0.89
YOLOv3	0.88	0.89	0.86	0.88
Proposed method	0.96	0.97	0.96	0.97

Table 3 shows that the proposed method significantly outperformed other well-known classification methods,

including Random Forest (RF), Support Vector Regression (SVR), and YOLOv3, across all key performance metrics. The proposed method achieved a precision of 0.96, recall of 0.97, F1-score of 0.96, and an overall accuracy of 0.97. In comparison, the Random Forest method obtained a precision of 0.89, recall of 0.87, F1-score of 0.87, and an accuracy of 0.84. The SVR method showed a precision of 0.91, recall of 0.89, F1-score of 0.89, and an accuracy of 0.89. YOLOv3, a widely used model for object detection, achieved a precision of 0.88, recall of 0.89, F1-score of 0.86, and an accuracy of 0.88. These results highlight the superiority of the proposed method in terms of precision, recall, F1-score, and overall accuracy. The enhanced performance can be attributed to the advanced preprocessing techniques and the robust ensemble of CNNs and segmentation models employed in the proposed method. This comprehensive evaluation underscores the effectiveness of the proposed method in accurately classifying various types of waste, making it a promising solution for automated waste management systems.

3.3. Parallel Processing Analysis

The efficiency and speed of the proposed waste classification method were significantly enhanced through the implementation of parallel processing techniques using an NVIDIA GPU GeForce RTX3060Ti with MATLAB 2023b. The performance improvements were evaluated by comparing the method's execution times and memory usage with and without parallel processing. The introduction of parallel processing demonstrated substantial reductions in computation time across various stages of the classification process, including normalization, feature extraction, encoding, and matching. Specifically, the element-wise GPU method utilized for parallel processing significantly accelerated these tasks by leveraging the vectorization of matrix and vector operations alongside gpuarray for parallel computation.

The results presented in Table 4 indicate that the GPU implementation reduced the normalization time from 0.1232 seconds to 0.0101 seconds (approximately 12 times faster), feature extraction and encoding time from 0.1421 seconds to 0.0023 seconds (approximately 62 times faster), and matching time from 0.1470 seconds to 0.0121 seconds (approximately 12 times faster). These improvements demonstrate the substantial impact of parallel processing on the efficiency of the system.

Table 4 Parallel processing analysis in terms of normalization, feature extraction, encoding and matching

Method	Implementation	Normalization (s)	Feature extraction and encoding (s)	Matching
Without Element-wise GPU	CPU	0.1232	0.1421	0.1470
With Element-wise GPU	GPU	0.0101	0.0023	0.0121

Table 5 Parallel processing analysis in terms of memory and execution time

Method	Implementation	Total size (MB)	Training time (Minutes)	Testing time/image (s)
Without Element-wise GPU	CPU	951.00	872.00	0.008
With Element-wise GPU	GPU	318.00	210.00	0.002

Moreover, Table 5 highlights the reduction in memory usage and execution time achieved through parallel processing. The total memory size required for the GPU implementation was reduced to 318 MB from 951 MB for the CPU implementation. Training time was significantly reduced from 872 minutes to 210 minutes (approximately 4 times faster), while the testing time per image decreased from 0.008 seconds to 0.002 seconds (4 times faster).

These results underscore the advantages of parallel processing in enhancing the speed and efficiency of the waste classification system. The ability to perform rapid and accurate image processing and classification in real-time is crucial for practical applications in high-throughput waste management facilities. The implementation of parallel processing not only accelerates the overall classification process but also enables the system to handle large volumes of waste images effectively, making it a robust solution for automated waste management.

4. Conclusion

This study presents a comprehensive and advanced waste classification system that leverages the power of deep learning techniques, specifically Convolutional Neural Networks (CNNs) and image segmentation models, to improve recycling processes and reduce human intervention. The system integrates a heterogeneous and hybrid ensemble of CNNs (MobileNetV2, AlexNet, VGG19, ResNet-50, and InceptionV3) and segmentation models (U-Net, Mask R-CNN, and DeepLabV3++), along with sophisticated image preprocessing techniques such as Fourier-based deblurring, curvelet-based empirical Wiener filtering, joint non-local means filtering, and reflection removal. These enhancements significantly improve image quality and classification accuracy. The decision-making process was optimized using a Reinforcement Learning-Differential Evolution (RL-DE) algorithm, which dynamically adjusts the contributions of each model to maximize classification accuracy. The implementation of parallel processing techniques on an NVIDIA GPU further improved the system's speed and efficiency, making it suitable for real-time applications. Experimental results demonstrated the system's exceptional

performance, achieving a precision of 0.96, recall of 0.97, F1-score of 0.96, and overall accuracy of 0.97. These results underscore the robustness and effectiveness of the proposed method in automated waste management.

Despite the promising results, the study has limitations regarding the dataset. Although diverse, the dataset may not encompass all possible variations of waste items encountered in real-world scenarios. This limitation could affect the model's generalizability and its ability to effectively handle novel waste items. Future research should focus on expanding the dataset to include more diverse and real-world waste images, which would improve the model's robustness and generalizability. Additionally, research could explore the application of this system to other areas of waste management, such as hazardous waste identification and sorting, to broaden its impact on environmental sustainability.

Acknowledgements

This study was conducted without the support of any grants or external funding.

REFERENCES

[1] J. Zhang and M. Zhu, "Collaborative governance of municipal solid waste in urban agglomerations: The case of Yangtze River Delta," Front Environ Sci, vol. 10, 2022, doi: 10.3389/fenvs.2022.999120.

[2] Y. Wei, M. Cui, Z. Ye, and Q. Guo, "Environmental challenges from the increasing medical waste since SARS outbreak," J Clean Prod, vol. 291, 2021, doi: 10.1016/j.jclepro.2020.125246.

[3] A. Xu, H. Chang, Y. Xu, R. Li, X. Li, and Y. Zhao, "Applying artificial neural networks (ANNs) to solve solid waste-related issues: A critical review," Waste Management, vol. 124. 2021. doi: 10.1016/j.wasman.2021.02.029.

[4] D. M. C. Chen, B. L. Bodirsky, T. Krueger, A. Mishra, and A. Popp, "The world's growing municipal solid waste: trends and impacts," Environmental Research Letters, vol. 15, no. 7, 2020, doi: 10.1088/1748-9326/ab8659.

[5] M. S. Rad et al., "A computer vision system to localize and classify wastes on the streets," in Lecture Notes in Computer Science (including subseries Lecture Notes in Artificial Intelligence and Lecture Notes in Bioinformatics), 2017. doi: 10.1007/978-3-319-68345-4_18.

[6] P. R. Yaashikaa et al., "A review on landfill system for municipal solid wastes: Insight into leachate, gas emissions, environmental and economic analysis," Chemosphere, vol. 309, 2022, doi: 10.1016/j.chemosphere.2022.136627.

[7] M. H. Ali, S. Zailani, M. Iranmanesh, and B. Foroughi, "Impacts of environmental factors on waste, energy, and resource management and sustainable performance," Sustainability (Switzerland), vol. 11, no. 8, 2019, doi: 10.3390/su11082443.

[8] Q. Duan and J. Li, "Classification of Common Household Plastic Wastes Combining Multiple Methods Based on Near-Infrared Spectroscopy," ACS ES and T Engineering, vol. 1, no. 7, 2021, doi: 10.1021/acsestengg.0c00183.

[9] S. P. Koko and K. Kusakana, "Impact of Corrosion in Carbon Steel Pipeline of Marine Wastewater Outfall during Electric Power Generation," in 2023 7th International Conference on Green Energy and Applications, ICGEA 2023, 2023. doi: 10.1109/ICGEA57077.2023.10125917.

[10] X. Cao et al., "Efficient pollutants removal and microbial flexibility under high-salt gradient of an oilfield wastewater treatment system," Science of the Total Environment, vol. 823, 2022, doi: 10.1016/j.scitotenv.2022.153619.

[11] S. Kaza, L. C. Yao, P. Bhada-Tata, and F. Van Woerden, What a Waste 2.0: A Global Snapshot of Solid Waste Management to 2050. 2018. doi: 10.1596/978-1-4648-1329-0.

[12] N. E. Johnson et al., "Patterns of waste generation: A gradient boosting model for short-term waste prediction in New York City," Waste Management, vol. 62, 2017, doi: 10.1016/j.wasman.2017.01.037.

[13] S. Zhang, Y. Chen, Z. Yang, and H. Gong, "Computer Vision Based Two-stage Waste Recognition-Retrieval Algorithm for Waste Classification," Resour Conserv Recycl, vol. 169, 2021, doi: 10.1016/j.resconrec.2021.105543.

[14] A. S. Girsang, A. D. Saputra, and V. Yanrie, "Performance Comparison between VGG16 and Inception V3 for Organic Waste and Recyclable Waste Classification," International Journal of Intelligent Systems and Applications in Engineering, vol. 11, no. 2, 2023.

[15] A. Pariatamby, M. S. Bhatti, and F. S. Hamid, "Waste Management in Developing Countries," 2019. doi: 10.4018/978-1-7998-0198-6.ch020.

[16] C. Srinilta and S. Kanharattanachai, "Municipal solid waste segregation with CNN," in Proceeding - 5th International Conference on Engineering, Applied Sciences and Technology, ICEAST 2019, 2019. doi: 10.1109/ICEAST.2019.8802522.

[17] J. Jose and T. Sasipraba, "An optimal model for municipal solid waste management using hybrid dual faster R-CNN," Environ Monit Assess, vol. 195, no. 4, 2023, doi: 10.1007/s10661-023-10984-6.

[18] A. Alsabei, A. Alsayed, M. Alzahrani, and S. Al-Shareef, "Waste Classification by Fine-Tuning Pre-trained CNN and GAN," International Journal of Computer Science & Network Security, vol. 21, no. 8, 2021.

[19] S. Poudel and P. Poudyal, "Classification of Waste Materials using CNN Based on Transfer Learning," in ACM International Conference Proceeding Series, 2022. doi: 10.1145/3574318.3574345.

[20] D. Gyawali, A. Regmi, A. Shakya, A. Gautam, and S. Shrestha, "Comparative Analysis of Multiple Deep CNN Models for Waste Classification," Apr. 2020, [Online]. Available: http://arxiv.org/abs/2004.02168

[21] S. Liang and Y. Gu, "A deep convolutional neural network to simultaneously localize and recognize waste types in images," Waste Management, vol. 126, 2021, doi: 10.1016/j.wasman.2021.03.017.

[22] O. Adedeji and Z. Wang, "Intelligent waste classification system using deep learning convolutional neural network," in

Procedia Manufacturing, 2019. doi: 10.1016/j.promfg.2019.05.086.

[23] J. Bobulski and M. Kubanek, "Waste Classification System Using Image Processing and Convolutional Neural Networks," in Lecture Notes in Computer Science (including subseries Lecture Notes in Artificial Intelligence and Lecture Notes in Bioinformatics), 2019. doi: 10.1007/978-3-030-20518-8_30.

[24] X. Meng, X. Tan, Y. Wang, Z. Wen, Y. Tao, and Y. Qian, "Investigation on decision-making mechanism of residents' household solid waste classification and recycling behaviors," Resour Conserv Recycl, vol. 140, 2019, doi: 10.1016/j.resconrec.2018.09.021.

[25] A. H. Vo, L. Hoang Son, M. T. Vo, and T. Le, "A Novel Framework for Trash Classification Using Deep Transfer Learning," IEEE Access, vol. 7, 2019, doi: 10.1109/ACCESS.2019.2959033.

[26] W. L. Mao, W. C. Chen, C. T. Wang, and Y. H. Lin, "Recycling waste classification using optimized convolutional neural network," Resour Conserv Recycl, vol. 164, 2021, doi: 10.1016/j.resconrec.2020.105132.

[27] S. L. Rabano, M. K. Cabatuan, E. Sybingco, E. P. Dadios, and E. J. Calilung, "Common garbage classification using mobilenet," in 2018 IEEE 10th International Conference on Humanoid, Nanotechnology, Information Technology, Communication and Control, Environment and Management, HNICEM 2018, 2018. doi: 10.1109/HNICEM.2018.8666300.

[28] N. Baras, D. Ziouzios, M. Dasygenis, and C. Tsanaktsidis, "A cloud based smart recycling bin for waste classification," in 2020 9th International Conference on Modern Circuits and Systems Technologies, MOCAST 2020, 2020. doi: 10.1109/MOCAST49295.2020.9200283.

[29] H. H. Chin, P. S. Varbanov, D. Fózer, P. Mizsey, J. J. Klemeš, and X. Jia, "Data-Driven Recyclability Classification of Plastic Waste," Chem Eng Trans, vol. 88, 2021, doi: 10.3303/CET2188113.

[30] Y. Chen, J. Sun, S. Bi, C. Meng, and F. Guo, "Multi-objective solid waste classification and identification model based on transfer learning method," J Mater Cycles Waste Manag, vol. 23, no. 6, 2021, doi: 10.1007/s10163-021-01283-8.

[31] Y. Chu, C. Huang, X. Xie, B. Tan, S. Kamal, and X. Xiong, "Multilayer hybrid deep-learning method for waste classification and recycling," Comput Intell Neurosci, vol. 2018, 2018, doi: 10.1155/2018/5060857.

[32] L. Yong, L. Ma, D. Sun, and L. Du, "Application of MobileNetV2 to waste classification," PLoS One, vol. 18, no. 3 March, 2023, doi: 10.1371/journal.pone.0282336.

[33] K. L. Li, "Analysis and suggestions on classification and recycling of urban domestic waste," in IOP Conference Series: Earth and Environmental Science, 2021. doi: 10.1088/1755-1315/647/1/012177.

[34] M. Schneider, R. Amann, and C. Mitsantisuk, "Waste object classification with AI on the edge accelerators," in 2021 IEEE International Conference on Mechatronics, ICM 2021, 2021. doi: 10.1109/ICM46511.2021.9385682.

[35] M. Malik et al., "Waste Classification for Sustainable Development Using Image Recognition with Deep Learning Neural Network Models," Sustainability (Switzerland), vol. 14, no. 12, Jun. 2022, doi: 10.3390/su14127222.

[36] Cchangcs, "Garbage classification."

[37] R. Pitakaso et al., "Artificial Intelligence in enhancing sustainable practices for infectious municipal waste classification," Waste Management, vol. 183, pp. 87–100, Jun. 2024, doi: 10.1016/j.wasman.2024.05.002.

[38] K. Sethanan et al., "Double AMIS-ensemble deep learning for skin cancer classification," Expert Syst Appl, vol. 234, 2023, doi: 10.1016/j.eswa.2023.121047.

[39] R. Pitakaso, C. Almeder, K. F. Doerner, and R. F. Hartl, "A MAX-MIN ant system for unconstrained multi-level lot-sizing problems," Comput Oper Res, vol. 34, no. 9, 2007, doi: 10.1016/j.cor.2005.09.022.

[40] Q. Fan, J. Yang, G. Hua, B. Chen, and D. Wipf, "A Generic Deep Architecture for Single Image Reflection Removal and Image Smoothing," in Proceedings of the IEEE International Conference on Computer Vision, 2017. doi: 10.1109/ICCV.2017.351.

[41] J. Yang, D. Gong, L. Liu, and Q. Shi, "Seeing Deeply and Bidirectionally: A Deep Learning Approach for Single Image Reflection Removal," in Lecture Notes in Computer Science (including subseries Lecture Notes in Artificial Intelligence and Lecture Notes in Bioinformatics), 2018. doi: 10.1007/978-3-030-01219-9_40